

## Slow Electrons Ejected from He by Fast Charged Particles\*

Yong-Ki Kim and Mitio Inokuti

Argonne National Laboratory, Argonne, Illinois 60439

(Received 25 September 1972)

An accurate differential ionization cross section for the ejection of zero-kinetic-energy electrons from He by fast charged particles is deduced by extrapolating the Born cross sections for discrete excitations, in the spirit of the quantum-defect theory. Recent electron-impact data by Grissom *et al.* for secondary electrons of almost zero kinetic energy are in excellent agreement with the theory. The electron-impact data by Peterson *et al.* for slow secondary electrons show trends consistent with the theory also. The proton-impact data by Rudd *et al.* are in better agreement with the theory than those by Stolterfoht.

### INTRODUCTION

Recently, a number of experiments on the secondary electrons from the ionization of He by fast electrons and protons have been reported in the literature.<sup>1-5</sup> These experiments provide the ionization cross-section differential in the kinetic energy of the secondary electrons. (When the incident particle is an electron, the slower of the two electrons that emerges after the collision is referred to as the secondary electron by convention.)

For slow (< 50 eV) secondary electrons, experimental uncertainty is serious when conventional energy analyzers are used. For instance, a discrepancy of a factor of 2 exists between the set of experimental data on He by Rudd *et al.*<sup>1</sup> and that by Stolterfoht<sup>2</sup> for slow electrons ejected by 300-keV protons (see Fig. 1). Grissom *et al.*<sup>4</sup> applied a trapped-electron method to detect only very-low-energy (< 1 eV) secondary electrons. The resulting cross section agrees well with theory as will be shown below.

According to the quantum-defect theory, cross sections for discrete excitations must connect smoothly into the corresponding continuum cross sections at the ionization thresholds, provided that the cross sections are normalized to the same energy scale.<sup>6</sup> The continuity of cross sections through thresholds has been utilized for the analysis of photoabsorption processes.<sup>7,8</sup> The same philosophy can be used also to analyze inelastic collisions of fast charged particles with atoms. In this paper we shall illustrate our point by using helium as an example. However, the method presented below can be extended, in principle, to any atom if sufficient data on discrete excitations are available. [See discussions concerning Eqs. (4.23) and (4.24) on pp. 327-328 of Ref. 9. The right-hand side of Eq. (4.23) should read  $[(\alpha^2/E)\dots]_{E=T}$ .

The asymptotic (for large incident-particle velocity) Born cross sections for discrete excita-

tions of He from its ground state are well known.<sup>10,11</sup> Therefore, one can obtain an accurate differential ionization cross section  $d\sigma/dE$  at the ionization

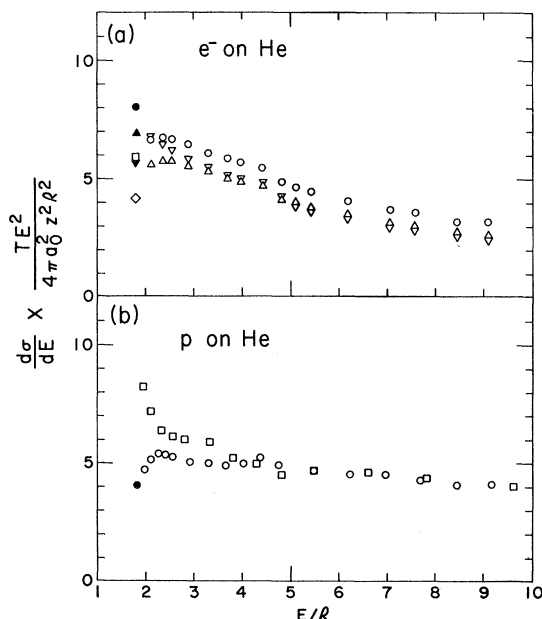


FIG. 1. The ratio of the differential ionization cross section  $d\sigma/dE$  of He to the Rutherford cross section as a function of the energy transfer  $E$ . For other mathematical symbols, see the text. The uncertainties in the experimental data quoted are 20 to 30%. (a) Ionization by electrons. The open circles, triangles, and inverted triangles represent experimental data by Peterson *et al.* (Ref. 3) with 2000-, 1000-, and 500-eV incident energy, respectively. The open square and diamond at the threshold stand for the experimental data with 500-eV incident energy by Grissom *et al.* (Ref. 4) and by Oda *et al.* (Ref. 5), respectively. The solid circle, triangle, and inverted triangle represent the Born cross section for 2000-, 1000-, and 500-eV incident energy, respectively. (b) Ionization by protons. The open squares and circles stand for the experimental data with 300-keV incident energy by Stolterfoht (Ref. 2) and by Rudd *et al.* (Ref. 1), respectively. The solid circle represents the Born cross section for the same incident energy.

threshold, where  $E$  is the energy transferred to the target, by extrapolating the discrete cross sections. The threshold value of  $d\sigma/dE$  thus obtained can be compared directly with the experiment by Grissom, Compton, and Garrett,<sup>4</sup> and also serves as a guide to judge the consistency of  $d\sigma/dE$  measured by Peterson, Beaty, and Opal,<sup>3</sup> by Rudd, Sautter, and Bailey,<sup>1</sup> and also by Stolterfoht<sup>3</sup> for slow secondary electrons.

### THEORY

The asymptotic form of the Born cross section for the excitation of an atom to a discrete state  $n$  by a (structureless) particle of charge  $ze$  and speed  $v$  is given by [Eqs. (4.18) and (4.20) of Ref. 9]

$$\sigma_n = \frac{4\pi a_0^2 z^2}{T/\mathcal{R}} \left[ \frac{f_n}{E_n/\mathcal{R}} \ln \left( \frac{4c_n T}{\mathcal{R}} \right) + \frac{\gamma_n}{T/\mathcal{R}} \right] \quad (1)$$

for an (optically) allowed transition, and

$$\sigma_n = \frac{4\pi a_0^2 z^2}{T/\mathcal{R}} \left( b_n + \frac{\gamma_n}{T/\mathcal{R}} \right) \quad (2)$$

for a forbidden transition, where  $a_0$  is the Bohr radius;  $\mathcal{R}$  is the Rydberg energy;  $T = \frac{1}{2}mv^2$ ,  $m$  being the *electron* mass (regardless of the type of incident particle);  $f_n$  is the optical oscillator strength;  $E_n$  is the excitation energy; and  $b_n$ ,  $c_n$ , and  $\gamma_n$  are constants evaluated from the wave functions of the target. The initial state is taken here to be the ground state, though the theory is applicable to any initial state.

The corresponding formula for the excitation to a continuum state is [Eq. (4.22) of Ref. 9]

$$\frac{d\sigma}{dE} = \frac{4\pi a_0^2 z^2}{T/\mathcal{R}} \left[ \frac{\mathcal{R}}{E} \frac{df}{dE} \ln \left( \frac{4c_E T}{\mathcal{R}} \right) + \frac{d\gamma}{dE} \frac{\mathcal{R}}{T} \right], \quad (3)$$

where  $E$ ,  $df/dE$ ,  $c_E$ , and  $d\gamma/dE$  are the continuum quantities which correspond to  $E_n$ ,  $f_n$ ,  $c_n$ , and  $\gamma_n$ , respectively. For a continuum state specified by  $E$  only, both optically allowed and forbidden transitions take place and  $c_E$  contains both contributions.

The continuity at the ionization threshold ( $E=B$ ) requires that [see Eqs. (11) and (12) of Ref. 10]

$$\lim_{n \rightarrow \infty} \frac{(n^*)^3 f_n \mathcal{R}}{2E_n} = \left( \frac{\mathcal{R}^2}{E} \frac{df}{dE} \right)_{E=B}, \quad (4)$$

$$\lim_{n \rightarrow \infty} \frac{1}{2} \left( \frac{(n^*)^3 f_n}{E_n/\mathcal{R}} \ln c_n + \sum' (n^*)^3 b_n \right) = \left( \frac{\mathcal{R}^2}{E} \frac{df}{dE} \ln c_E \right)_{E=B}, \quad (5)$$

where  $\sum' (n^*)^3 b_n$  here stands for the sum over all different angular momenta except for the  $P$  channel, and

$$\lim_{n \rightarrow \infty} \frac{1}{2} \sum (n^*)^3 \gamma_n = \mathcal{R} \left( \frac{d\gamma}{dE} \right)_{E=B}, \quad (6)$$

where, in this case, the sum includes all angular momenta.

The values of  $f_n \mathcal{R}/E_n$ ,  $\mathcal{R} f_n (\ln c_n)/E_n$ , and various  $b_n$  for large  $n$  as functions of  $n^*$  ( $=n + \text{quantum defect}$ ) are given in Table I of Ref. 10 for the excitations of He. From Ref. 10 we have

$$\lim_{n \rightarrow \infty} (n^*)^3 f_n \mathcal{R}/2E_n = 0.506 \quad (7)$$

in excellent agreement with the continuum results extrapolated from the calculation of Jacobs<sup>12</sup>; and

$$\lim_{n \rightarrow \infty} \frac{1}{2} \left( \frac{(n^*)^3 f_n}{E_n/\mathcal{R}} \ln c_n + \sum' (n^*)^3 b_n \right) = -0.769. \quad (8)$$

[Actually, the above value incorporates a slight improvement upon the data of Ref. 10. On the basis of the calculation by Vanderpoorten,<sup>13</sup> we now estimate  $b_{n^1F} + b_{n^1G} + \dots = (0.134n^{-3} - 1.33n^{-5}) \times 10^{-2}$ . For the more important transitions (i. e., to the  $^1P$ ,  $^1S$ , and  $^1D$  states), the data of Ref. 10 remain intact.]

The values of  $\gamma_n$  for allowed transitions depend on the mass of the incident particle. We use the notation  $\gamma^{(e)}$  for electron or positron, and  $\gamma^{(\infty)}$  for heavy particles such as mesons, protons, and  $\alpha$  particles. Then, from Ref. 11 we have

$$\lim_{n \rightarrow \infty} \frac{1}{2} \sum (n^*)^3 \gamma_n^{(e)} = -0.175 \quad (9)$$

and

$$\lim_{n \rightarrow \infty} \frac{1}{2} \sum (n^*)^3 \gamma_n^{(\infty)} = +0.283. \quad (10)$$

The values in Eqs. (9) and (10) actually include contributions from transitions to the  $^1P$ ,  $^1S$ , and  $^1D$  states *only*. Transitions to the  $^1F$ ,  $^1G$ , and higher angular-momentum states have vanishing  $\gamma_n$  because of selection rules that are apparent from Eqs. (3.14) and (4.19) of Ref. 9.

For incident electrons, additional corrections must be made for the exchange effect. We use the exchange correction based on the Mott formula [as given in Eq. (55) of Ref. 11]

$$\frac{d\sigma_{\text{exch}}}{dE} = \frac{4\pi a_0^2 \mathcal{R}^2 N}{T} \left( \frac{1}{(T-W)^2} - \frac{1}{E(T-W)} \right), \quad (11)$$

where the number of atomic electrons  $N=2$  for He, and  $W$  is the kinetic energy of the secondary electron.

With Eqs. (4)–(11), Eq. (3) becomes

$$\left(\frac{d\sigma}{dE} \frac{T}{4\pi a_0^2 z^2}\right)_{E=B} = 0.506 \ln\left(\frac{4T}{R}\right) - 0.769 + \frac{R}{T} \times \begin{cases} -0.175 & \text{for } e^+, \\ -0.175 - 2R\left(\frac{1}{B} - \frac{1}{T}\right) & \text{for } e^-, \\ +0.283 & \text{for heavy particles.} \end{cases} \quad (12)$$

For He,  $B = 24.58 \text{ eV} = 1.807R$  and some numerical results from Eq. (12) are given in Table I.

Differential ionization cross sections of He have been calculated by Bell and Kingston,<sup>14</sup> and more recently by Omidvar, Kyle, and Sullivan.<sup>15</sup> Both calculations explicitly use ground-state and continuum wave functions. The cross section at the threshold calculated by Bell and Kingston for 300-keV protons agrees with our value within a few percent, while those by Omidvar *et al.* for fast protons and electrons are 10 to 15% lower than our values.

#### COMPARISON WITH EXPERIMENT

Our theory gives the Born cross section for single ionization of He leaving the ion in its ground state. None of the experiments mentioned in this paper, except for that by Oda *et al.*,<sup>5</sup> monitors the energy loss of the incident particle, and the measured cross section is the sum of the cross sections leaving the He ion in various states, including doubly ionized states. An estimate of the combined contribution from the excited-ion states by Oldham and Miller<sup>16</sup> is  $\sim 7\%$ , and our estimate from the accurate optical oscillator strengths in Refs. 12 and 17 is  $\sim 3\%$ , certainly far less than the uncertainties in the experiments. Therefore, we shall ignore the effects of the excited-ion states in the following discussion.

The experimental data by Grissom, Compton, and Garrett<sup>4</sup> with 500-eV incident electrons can be compared directly to the cross sections given by Eq. (12). Their value in Table I is in excellent agreement with the theoretical value [see also Fig. 1(a)].

The data by Peterson, Beaty, and Opal<sup>3</sup> with fast electrons (500–2000 eV) do not cover the ionization threshold. Nevertheless, it is clear from Fig. 1(a) that the trend observed in their data is

such that an extrapolation to the ionization threshold would yield cross sections consistent with the theory within the experimental uncertainty of  $\pm 25\%$ . Figure 1(a) also suggests that the cross section for the 500-eV incident electron by Peterson *et al.*<sup>3</sup> is too large, while those for 1- and 2-keV electrons are too small. This tendency also explains an irregular dependence on incident energy observed in the angular distribution of the secondary electrons (see Fig. 2 of Ref. 18). Actually, Peterson *et al.*<sup>3</sup> measured the angular distributions and integrated them to obtain  $d\sigma/dE$ .

The ordinate in Fig. 1 is the ratio of  $d\sigma/dE$  to the Rutherford cross section<sup>19</sup>

$$\left(\frac{d\sigma}{dE}\right)_{\text{Ruth}} = \frac{4\pi a_0^2 z^2 R^2}{TE^2}, \quad (13)$$

and the ratio should approach  $N=2$  asymptotically (for large energy transfer) for proton-impact data.

When the incident particle is an electron, the indistinguishability of the incident and ejected electron makes  $d\sigma/dE$  (as a function of the kinetic energy  $W$  of the secondary electron) symmetric with respect to the axis at  $E = \frac{1}{2}(T+B)$ . One can use this symmetry to obtain the value of  $d\sigma/dE$  at  $E=B$  by measuring the cross section for secondary electrons of kinetic energy  $W=T-B$ . Such a measurement was done by Oda *et al.*<sup>5</sup> with 500-eV incident electrons, and their result in Table I is somewhat lower than the Born cross section. The experimental value by Oda *et al.*<sup>5</sup> is low, probably because their measurement excludes the electrons emerging in the extreme forward direction ( $< 5^\circ$ ).

As for the proton-impact experiments,<sup>1,2</sup> the highest incident energy used is 300 keV. The speed of the incident particle that appears through  $T$  in Eqs. (1) and (2) is an important variable for the validity of the first Born approximation, and

TABLE I. The differential ionization cross section  $d\sigma/dE$  of He for zero-kinetic-energy secondary electrons.

Incident particle	Incident energy	$T/R$	Theory (present work) $d\sigma/dE$ in $\text{cm}^2/\text{eV}$	Experiment $d\sigma/dE$ in $\text{cm}^2/\text{eV}$
$e^-$	2000 eV	147.0	$4.31 \times 10^{-19}$	
	1000 eV	73.5	$7.35 \times 10^{-19}$	
	500 eV	36.8	$1.21 \times 10^{-18}$	$1.28 \times 10^{-18} \pm 30\%^a$ $0.90 \times 10^{-18} \pm 20\%^b$
$p$	300 keV	12.0	$2.61 \times 10^{-18}$	

<sup>a</sup>Reference 4.

<sup>b</sup>Reference 5.

a 300-keV proton is not fast enough from this viewpoint. However, the heavy mass of the proton makes its trajectory well localized, a condition favorable for the application of the impact-parameter approximation which remains valid at lower velocities.<sup>20</sup> Furthermore, the experiments in Refs. 1 and 2 do not measure the zero-kinetic-energy secondary electrons, and we can only discuss an apparent trend in their data for slow secondary electrons.

The asymptotic Born cross section for 300-keV incident protons agrees better with the experimental data near the threshold by Rudd, Sautter, and Bailey<sup>1</sup> than those by Stolterfoht<sup>2</sup> [Fig. 1(b)]. However, the ratio  $(d\sigma/dE)/(d\sigma/dE)_{\text{Ru th}}$  derived from Ref. 1 approaches the threshold with a slope too large to connect smoothly with corresponding theoretical data for discrete excitations.<sup>21</sup> At the ionization threshold, the theoretical ratio has negative slopes for incident electron energies shown in Fig. 1(a) and positive slopes for proton energies shown in Fig. 1(b). The magnitudes of the slope depend on  $T$ , and for the ionization of He a negative slope is expected at the threshold for large  $T$  regardless of the type of the incident particle. Proton-impact data on the ionization of He by faster protons ( $>1$  MeV) are desirable to check the validity of the Born cross sections with confidence.

Because Eq. (12) is a truncated power series in  $1/T$ , the magnitude of the last term (with  $\mathcal{R}/T$ ) on

the right-hand side relative to the sum of the preceding two terms would indicate the importance of the higher-order terms not included in Eq. (12). For protons, the last term contributes less than 4% to the differential cross section at  $T/\mathcal{R}=10$ . For high  $T$ , say  $>50\mathcal{R}$ , the cross section given by Eq. (12) should be adequate for normalization of experimental data. The normalization of electron-impact data may utilize also the reflection symmetry of the differential cross section; in other words, Eq. (12) could be applied to the cross section for the energy loss of  $B=24.58$  eV from the *primary* electron.

The foregoing treatment is simple because an overwhelming majority of ionization events results in the  $\text{He}^+$  ground state. In general, an ion may be left in one of the alternative states slightly differing in energy (e.g., the  $J=\frac{1}{2}$  and  $\frac{3}{2}$  states of other rare-gas ions). In such cases, an adaptation to the multichannel quantum-defect theory<sup>6-8</sup> would be necessary.

#### ACKNOWLEDGMENTS

We thank Dr. R. N. Compton for communicating the experimental data in Ref. 4 prior to publication, and to Professor N. Oda for providing us with the details of the experiment quoted in the text (Ref. 5). We also thank Professor U. Fano for valuable comments.

\*Work performed under the auspices of the U.S. Atomic Energy Commission.

<sup>1</sup>M. E. Rudd, C. A. Sautter, and C. L. Bailey, *Phys. Rev.* **151**, 20 (1966).

<sup>2</sup>N. Stolterfoht, *Z. Phys.* **248**, 81 (1971).

<sup>3</sup>W. K. Peterson, E. C. Beaty, and C. B. Opal, *Phys. Rev. A* **5**, 712 (1972); C. B. Opal, E. C. Beaty, and W. K. Peterson, *At. Data* **4**, 209 (1972).

<sup>4</sup>J. T. Grissom, R. N. Compton, and W. R. Garrett, *Phys. Rev. A* **6**, 977 (1972).

<sup>5</sup>N. Oda, F. Nishimura, and S. Tahira, *J. Phys. Soc. Jap.* **33**, 462 (1972); also, N. Oda (private communication, 1972).

<sup>6</sup>M. J. Seaton, *Proc. Phys. Soc. Lond.* **88**, 801 (1966); *Proc. Phys. Soc. Lond.* **88**, 815 (1966).

<sup>7</sup>D. L. Moores, *Proc. Phys. Soc. Lond.* **88**, 843 (1966).

<sup>8</sup>K. T. Lu, *Phys. Rev. A* **4**, 579 (1971).

<sup>9</sup>M. Inokuti, *Rev. Mod. Phys.* **43**, 297 (1971).

<sup>10</sup>M. Inokuti and Y.-K. Kim, *Phys. Rev.* **186**, 100 (1969).

<sup>11</sup>Y.-K. Kim and M. Inokuti, *Phys. Rev. A* **3**, 665 (1971).

<sup>12</sup>V. Jacobs, *Phys. Rev. A* **3**, 289 (1971).

<sup>13</sup>R. Vanderpoorten, *Physica (Utr.)* **48**, 254 (1970).

<sup>14</sup>K. L. Bell and A. E. Kingston, *J. Phys. B* **2**, 653 (1969).

<sup>15</sup>K. Omidvar, H. L. Kyle, and E. C. Sullivan, *Phys. Rev. A* **5**, 1174 (1972).

<sup>16</sup>W. J. B. Oldham, Jr. and B. P. Miller, *Phys. Rev. A* **3**, 942 (1971).

<sup>17</sup>V. L. Jacobs and P. G. Burke, *J. Phys. B* **5**, L67 (1972).

<sup>18</sup>Y.-K. Kim, *Phys. Rev. A* **6**, 666 (1972).

<sup>19</sup>The usual form of the Rutherford formula is for an unbound target particle and is expressed in terms of the momentum transfer. Equation (13), in which  $E$  includes the binding energy of the target electron, constitutes a departure from the original spirit of the Rutherford formula.

<sup>20</sup>See for instance, Sec. 4.4, Ref. 9.

<sup>21</sup>The quantum-defect theory requires that the quantities on both sides of Eq. (4) be equal both in magnitude (with sign) and slope, when they are considered as functions of the energy transfer. The same requirements hold also for Eqs. (5) and (6), respectively.